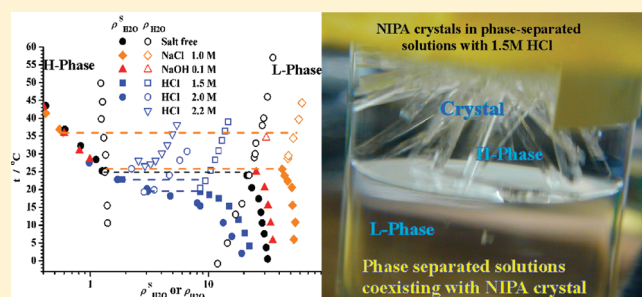


Effects of Ions on the Solubility Transition and the Phase-Separation of *N*-Isopropylacrylamide in Water

Shigeo Sasaki* and Satoshi Okabe

Department of Chemistry, Faculty of Sciences, Kyushu University, 33 6-10-1 Hakozaki, Higashi-ku, Fukuoka 812-8581, Japan

ABSTRACT: The effects of NaCl, NaOH, and HCl on the solubility transition and the phase-separation of *N*-isopropylacrylamide (NIPA) were investigated for the purpose of clarifying the physicochemical mechanism of salting-out and salting-in phenomena. The discrete change in the solubility of NIPA in the salt-free water at the solubility transition (reported in *J. Phys. Chem. B* 2010, 114, 14995–15002) decreased with the addition of HCl and disappeared in the HCl solutions at concentrations higher than 2 M, while it increased with additions of NaOH and NaCl. A difference in NIPA concentration between the phase-separated solutions decreases with the addition of HCl and increases with additions of NaOH and NaCl. Partition coefficients of HCl in the phase-separated NIPA-rich solutions are higher than those in the NIPA poor solutions, while partition coefficients of NaCl and NaOH between the NIPA-rich and -poor solutions have trends opposite to those of HCl. The present results clearly indicate that the HCl favors the dehydrated NIPA and stabilizes the H₂O-poor state of the NIPA molecule more than NaCl.



1. INTRODUCTION

Recent observations of hydrogen-bond structure in aqueous solutions of salts^{1,2} have cast doubt on the established explanation for the Hofmeister series^{3,4} that the ion species arranged in order of the ability to salt-out or salt-in the protein from an aqueous solution can be characterized by the capacity to “make” or “break” water structure. It has been newly proposed⁵ that the dehydration of a solute molecule leading to salting-out in water is caused by specific ion binding, the degree of which depends on the relative polarizability of the binding state. The salt effects on the behavior of thermal responsive poly(*N*-isopropylacrylamide) has been explained on the basis of interactions of anions with a macromolecule and a hydration shell.^{6–8} The volume phase transition of poly(*N*-isopropylacrylamide) gel in water^{9,10} caused by the hydration–dehydration of the hydrophobic isopropyl group of the side chain^{11–13} also changes with the addition of salt. It has been inferred, however, from the low distribution coefficients of salt inside a collapsed poly(*N*-isopropylacrylamide) gel¹⁴ that ion binding to the gel is unlikely to occur. It can be said that ion binding alone is insufficient to explain the physicochemical mechanism of the Hofmeister series of ions.

It is well-known that the hydration–dehydration of a hydrophobic entity located near the amide groups of biomaterials plays a very important role in the association–dissociation of biomacromolecules in biological cells.¹⁵ In order to gain insight into the thermodynamic mechanism of the hydration–dehydration^{16,17} in the system having hydrophobic residues with nearby amide groups, *N*-isopropylacrylamide (NIPA) in H₂O has been investigated and found to exhibit very interesting features such as solubility transition, liquid–liquid phase separation, and glass formation.¹⁸ In aqueous media, the interactions of the hydrogen

bond networks of H₂O molecules with the amide group and the hydrophobic residue play essential roles in the hydration–dehydration of NIPA. It has been inferred that the C=O and NH of the amide group form hydrogen bonds to a H₂O molecule and that the isopropyl group is surrounded by a hydrogen bond network consisting of a few tens of H₂O molecules. The thermodynamic balance between the entropy loss and the enthalpy gain accompanied by the hydrogen bond formation mentioned above determines the solubility and the phase-separated state of NIPA molecules. We have revealed that the 1:1 complex of NIPA and H₂O molecules behaves thermodynamically something like one liquid molecule and easily forms the glass in freezing the thermal motion with cooling, and that the formation of a hydrogen bond network around the isopropyl group leads to a large enthalpy gain for stabilizing the H₂O-rich state in the solution.¹⁸

In the present experiments, the effects of NaCl, NaOH, and HCl on the solubility transition and the phase-separation of NIPA in water were clarified. The discrete change in the solubility of NIPA in the salt-free water at the solubility transition¹⁸ decreased with the addition of HCl and disappeared in the HCl solutions at concentrations higher than 2M, while it increased with additions of NaOH and NaCl. The difference in NIPA concentration between the phase-separated solutions decreases with the addition of HCl and increases with additions of NaOH and NaCl. Partition coefficients of HCl in the phase-separated NIPA-rich solutions are higher than those in the

Received: August 7, 2011

Revised: October 1, 2011

Published: October 05, 2011

NIPA-poor solutions, while partition coefficients of NaCl and NaOH between the NIPA-rich and -poor solutions have trends opposite to those of HCl. The concentrations of NaOH and NaCl in the phase-separated H₂O-rich solutions are, respectively, about 100 times and 5 times those in the NIPA-rich solutions. The present results clearly indicate that the Na cation favors the hydrated state of NIPA molecules and that the Cl anion favors the dehydrated state of NIPA molecules in the aqueous solution.

2. EXPERIMENTAL METHODS

The NIPA monomer (Kojin Co. Tokyo) was recrystallized from toluene/hexane, and water was double distilled.

The experiments of phase separation were carried out as follows: When the needle-like NIPA crystals were mixed with NaCl, HCl, or NaOH aqueous solution in a glass tube at 30 °C, stoppered, and shaken, the liquid was initially turbid, but separated into two phases of transparent solutions upon standing at the given temperature, which was controlled within 0.1 °C using a thermo-regulator system (Thermo-regulator NCB-1200, Eyela Inc., Japan). The concentrations of NaCl, HCl, or NaOH in the NIPA solutions hereafter are defined as the molarity of their aqueous parts (mol/dm³ H₂O) and will be denoted by C_{NaCl} , C_{HCl} , and C_{NaOH} . After equilibrating between the phases for a period longer than 12 h, the solutions in the upper and lower parts were carefully withdrawn separately, and their H₂O/NIPA mole ratios, $\rho_{\text{H}_2\text{O}}$, were evaluated from the area ratios of the ¹H NMR peak for the H₂O protons (ca. 4.5 ppm) and the methyl protons of NIPA (ca. 1.2 ppm). Upper (NIPA-rich) and lower (H₂O-rich) parts of the phase-separated solutions will be called the H-phase and the L-phase hereafter. The ¹H NMR spectra were obtained on a Bruker AVANCE III 600 NMR spectrometer. We determined C_{HCl} and C_{NaCl} of the phase-separated solutions from conductometric titration with adding AgNO₃. We estimated C_{NaOH} of the phase-separated solutions from the atomic absorption data at a wavelength of 589 nm (atomic absorption spectrophotometer AA-6300 Shimadzu, Japan). The boundary at which one phase separates into two phases in the solutions consisting of HCl was determined by a cloud point measurement for a series of solutions with different NIPA concentrations. The cloud point was determined by monitoring the turbidity of the solution contained in glass tubes with a laser light ($\lambda = 532$ nm) while the temperature of the solution was raised or reduced step by step (0.5 °C step) with stirring. The turbidity observation was made during 2 h at a given temperature. The reversibility of the phase separation was confirmed by the coincidence of the temperatures at which the turbidity increased in heating and diminished in cooling. The H₂O/NIPA mole ratio of the solution ($r_{\text{H}_2\text{O}}$) prepared for the cloud point experiment can be regarded as one of the phase-separated solutions' $\rho_{\text{H}_2\text{O}}$ values at the cloud temperature.

The $r_{\text{H}_2\text{O}}$ value of the solution equilibrating with the NIPA solid will be denoted as $\rho_{\text{H}_2\text{O}}^{\text{S}}$. The measurement of ¹H NMR spectroscopy for the solution separated from the solid was made, and the $\rho_{\text{H}_2\text{O}}^{\text{S}}$ value of the solution was obtained from the area ratio of a proton peak of H₂O to a proton peak of methyl as described before. The dissolution experiment as given below was also carried out for the saturated solution, which was very difficult to separate from the solid. A mixture of NIPA and the aqueous salt solution with a given $r_{\text{H}_2\text{O}}$ was placed in a glass tube, sealed, heated to 50 °C with shaking, and then cooled to 20 °C for a period longer than 1 h with shaking to ensure the precipitation of

NIPA crystals. The temperature t_{d} at which the crystalline solid completely dissolved into the solution was determined by the clarification of the turbid solution in raising the temperature step by step (0.5 °C step). The observation of the dissolution was made with stirring the solution for a period longer than 2 h. The $r_{\text{H}_2\text{O}}$ value can be regarded as a $\rho_{\text{H}_2\text{O}}^{\text{S}}$ value at t_{d} .

It should be mentioned that small peaks identified as the protons of isopropylamine and acrylic-acid were observed in the ¹H NMR spectra of the NIPA in the 1 M NaOH solution but not in the 1 M NaCl solution nor the 2.2 M HCl solution. This indicates that hydrolysis of the amide group of the NIPA molecule is promoted by the interaction between the amide proton and hydroxyl ions in the solution, which induces concentrating changes of electrons' orbits related to the amide bond and H₂O molecules^{19,20} and hydrolyzes the amide. No observation of the hydrolysis of NIPA in the NaCl solutions suggests that Na⁺ ions distributed nearby the carbonyl oxygen of the amide group²¹ could not promote the hydrolysis. In the present experiments, the phase behavior of NIPA in the 0.1 M NaOH solutions standing still for one day, during which hydrolysis was not detected, was examined for avoiding the effect of hydrolysis. It should also be mentioned that NIPA molecules were slowly polymerized in the highly concentrated HCl solutions at higher temperatures after standing still for longer than 2 days. The polymerization was confirmed by the observation of very small peaks derived from the NIPA polymer in the ¹H NMR spectra. The turbid polymerized NIPA solution at a temperature above 34 °C became transparent at a temperature below it as was expected. This indicates that the interaction of the hydronium ion (hydrated proton) with the vinyl residue of the NIPA molecule promotes the polymerization of NIPA. The hydronium oxygen lone pair²¹ could induce the initiation of the polymerization of NIPA. Polymerizations of NIPA molecules were also observed in highly concentrated HNO₃ and HBr aqueous solutions, which were confirmed by the turbidity of the solutions due to the collapsing NIPA polymers at a temperature above 34 °C. In the present experiments, the observation of phase behavior of NIPA in HCl solution was made within 2 days after preparing the solution to avoid the effects of polymerization.

3. RESULTS

3.1. Solubility Transition Behavior of NIPA in Solutions of NaCl, NaOH, and HCl. Figure 1 shows that the $\rho_{\text{H}_2\text{O}}^{\text{S}}$ values of NIPA in the solutions with $C_{\text{NaCl}} = 1$ M at temperatures below 25.7 °C (orange filled diamonds) are greater than the $\rho_{\text{H}_2\text{O}}^{\text{S}}$ values of NIPA in the salt-free solution (black filled circles). However, the $\rho_{\text{H}_2\text{O}}^{\text{S}}$ values at temperatures above 36.0 °C are less than 0.6 and follow almost the same $t-\rho_{\text{H}_2\text{O}}^{\text{S}}$ diagram as that of the H-phase solution in the salt-free case. At temperatures below 25.7 °C and above 36.0 °C, we observed the homogeneous mixtures of 1 M NaCl solutions coexisting with the NIPA solid. At temperatures between 25.7 and 36.0 °C, however, the 1 M NaCl solution, in which an excess amount of NIPA solid was dissolved, separated into two solutions: a solution with a higher $\rho_{\text{H}_2\text{O}}$ (a L-phase regime) and a higher NaCl concentration than 1M, and a solution with a lower $\rho_{\text{H}_2\text{O}}$ (a H-phase regime) and a lower NaCl concentration than 1M. The existence of three-phases (coexistence of one solid phase and two solution phases) with one degree of freedom in the three-component system (NIPA, H₂O, and NaCl) is allowed at equilibrium by the Gibbs' phase rule. The $\rho_{\text{H}_2\text{O}}^{\text{S}}$ values of NIPA in the solutions with $C_{\text{NaCl}} = 1$ M at

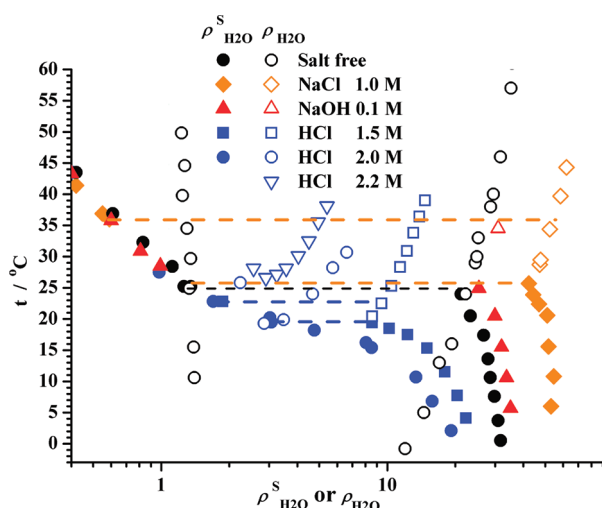


Figure 1. Phase diagram of NIPA in salt-free (black circle), 1 M NaCl (orange diamond), 0.1 M NaOH (red triangle), 1.5 M HCl (blue square), 2.0 M HCl (blue circle), and 2.2 M HCl (blue inverse triangle) aqueous solutions. Filled symbols and open circles represent the $t-\rho_{\text{H}_2\text{O}}^{\text{S}}$ relation of the saturated solution and the $t-\rho_{\text{H}_2\text{O}}$ relation of the phase separation boundary, respectively. The horizontal black dashed line indicates the solubility transition of solid NIPA in the salt-free solutions. Two liquid and NIPA solid coexisting phases are observed in the regions between the pairwise horizontal dashed lines (blue: 1.5 M HCl; orange: 1 M NaCl).

just above 36.0 °C and at just below 25.7 °C, respectively, are 0.59 and 42.7. The solubility behavior of NIPA described above is different from that in the salt-free aqueous solution, which exhibits the abruptly changing $\rho_{\text{H}_2\text{O}}^{\text{S}}$ from 1.3 to 21 at 25 °C.

The red filled triangles in Figure 1 demonstrate that the $\rho_{\text{H}_2\text{O}}^{\text{S}}$ values of NIPA in the 0.1 M NaOH solutions at temperatures lower than 25 °C are greater than the $\rho_{\text{H}_2\text{O}}^{\text{S}}$ values in the salt-free case and that the $\rho_{\text{H}_2\text{O}}^{\text{S}}$ values at temperatures higher than 25 °C follow almost the same $t-\rho_{\text{H}_2\text{O}}^{\text{S}}$ diagram as that of the H-phase solution in the salt-free case. The tendency of $\rho_{\text{H}_2\text{O}}^{\text{S}}$ change with adding NaOH is qualitatively very similar to the tendency of change with adding NaCl as described in the previous paragraph. It can be said that the existence of Na^+ ions in the solution reduces the NIPA solubility in the L-phase solution.

The blue filled squares in Figure 1 represent the temperature dependence of $\rho_{\text{H}_2\text{O}}^{\text{S}}$ in the 1.5 M HCl solutions, which is different from the temperature dependence of $\rho_{\text{H}_2\text{O}}^{\text{S}}$ presented by the black filled circles. The $\rho_{\text{H}_2\text{O}}^{\text{S}}$ values at the low temperatures are less than those in the salt-free case, and a range of the diagram at the high temperature extends to a point, $\rho_{\text{H}_2\text{O}}^{\text{S}} = 1.9$ and $t = 22.8$ °C. The overall trend of the $t-\rho_{\text{H}_2\text{O}}^{\text{S}}$ diagram at high temperatures is, however, almost same as that in the salt-free case. The transition occurs between the points ($\rho_{\text{H}_2\text{O}}^{\text{S}} = 1.9$, $t = 22.8$ °C) in the H-phase regime and ($\rho_{\text{H}_2\text{O}}^{\text{S}} = 8.3$, 18.5 °C) in the L-phase regime. The gap between a maximum $\rho_{\text{H}_2\text{O}}^{\text{S}}$ value in the H-phase regime and a minimum $\rho_{\text{H}_2\text{O}}^{\text{S}}$ value in the L-phase regime decreases with an increase in HCl concentration of the solution and is reduced to zero at $C_{\text{HCl}} = 2$ M, as demonstrated by blue filled circles in Figure 1. The solubility transition of NIPA solid disappears in the solutions with higher HCl concentrations than 2 M. The mixture of 1.5 M HCl solution coexisting with NIPA solid at temperatures between 18.5 and 22.8 °C was found

Table 1. Concentrations of NaCl, C_{NaCl} , in the Phase-Separated NIPA Solutions Obtained upon Dissolving the NIPA Solid in the Aqueous Solutions with Various NaCl Concentrations, C_{NaCl}^*

temperature °C	phase	$\rho_{\text{H}_2\text{O}}$	C_{NaCl}/M	phase	$\rho_{\text{H}_2\text{O}}$	C_{NaCl}/M	$C_{\text{NaCl}}^*/\text{M}$
28.7	L	34.6	0.56	H	1.18	0.13	0.5
	L	51.4	1.11	H	1.06	0.22	1
29.5	L	29.7	0.32	H	1.26	0.082	0.2
	L	52.3	1.11	H	1.05	0.24	1
34.4	L	27.3	0.12	H	1.32	0.034	0.1
	L	38.8	0.54	H	1.19	0.13	0.5
	L	57.2	1.14	H	1.06	0.22	1
	L	81.3	1.62	H	0.98	0.31	1.5
39.7	L	42.1	0.56	H	1.18	0.12	0.5
	L	62.3	1.1	H	1.0	0.26	1
44.3	L	45.4	0.57	H	1.18	0.12	0.5
	L	65.5	1.11	H	1.06	0.21	1

to separate into two solutions: a solution with lower concentrations of NIPA and HCl; a solution with higher concentrations of them. The present experiment exhibits that the dissolution of excess NIPA solids in the 1.5 M HCl aqueous solutions at temperatures between 18.5 and 22.8 °C cannot be realized without separating the solution into two solutions with HCl concentrations higher and lower than 1.5 M.

3.2. Phase Separation Behavior of NIPA in Solutions of NaCl, NaOH, and HCl. The black open circles in Figure 1 show the phase-separation boundaries of the salt-free aqueous NIPA solutions. We have reported¹⁸ that the metastable phase-separated state of NIPA solutions at temperatures much below 25 °C, say 5 °C, is maintained for a few days. We found in the present experiments, however, that the NIPA crystals precipitated from the metastable phase-separated NIPA solution with $C_{\text{NaCl}} = 1$ M standing still for 1 h, even at 25 °C. The supersaturated state at 25 °C is more destabilized by the addition of NaCl to the solutions.

The concentrations of NaCl in the phase-separated NIPA solutions obtained with dissolving the NIPA solid in the NaCl aqueous solutions are tabulated in Table 1. The concentrations of NaCl in the L-phase solutions are 4–5 times higher than those in the H-phase solutions. The H-phase solution has a much weaker affinity for NaCl than the L-phase solution. For clarifying the affinity correlation among NIPA, H_2O , and NaCl, the C_{NaCl} values are plotted against $\rho_{\text{H}_2\text{O}}$. An approximate relation of $C_{\text{NaCl}} = A \ln \rho_{\text{H}_2\text{O}}/\rho_0$ is found in the $C_{\text{NaCl}}-\rho_{\text{H}_2\text{O}}$ plots, as shown in Figure 2. The A values are obtained as -1 for the H-phase solution and 1.39 for the L-phase solution. It is interesting that the ρ_0 value for the H-phase, which can be a $\rho_{\text{H}_2\text{O}}$ value of the salt-free H-phase solution, seems to be constant (about 1.35) irrespective of the temperatures. The $\rho_{\text{H}_2\text{O}}$ values of salt-free H-phase solutions shown by black open circles in Figure 1 could be regarded as invariant (about 1.3) between 29 and 44 °C, although they decrease slightly with an increase in temperature.

The $\rho_{\text{H}_2\text{O}}^{\text{S}}$ value and the $\rho_{\text{H}_2\text{O}}$ value at the solubility transition temperature coincide with each other as observed in the case of salt-free solution shown in Figure 1. For examining the existence of $\rho_{\text{H}_2\text{O}}^{\text{S}} = \rho_{\text{H}_2\text{O}}$ in the case of the solution with $C_{\text{NaCl}} = 1$ M, the $\rho_{\text{H}_2\text{O}}$ values of the L-phase solutions are estimated as a function

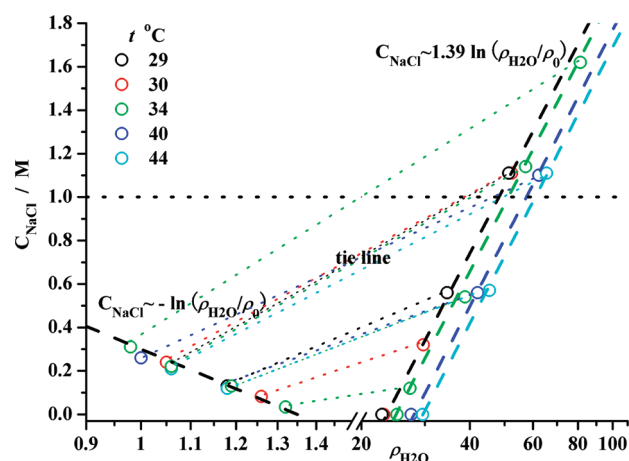


Figure 2. Distributions of NaCl and H₂O between the separated phases of the solutions obtained in dissolving the NIPA solid in the NaCl aqueous solutions with various concentrations at various temperatures indicated in the panel. Data are shown in Table 1. Tie lines are represented by dotted lines. Dashed lines represent curves given by $C_{\text{NaCl}} = A \ln \rho_{\text{H}_2\text{O}} \approx \rho_0$.

Table 2. Concentrations of NaOH, C_{NaOH} , in the Phase-Separated NIPA Solutions Obtained upon Dissolving the NIPA Solid in 1 M NaOH Aqueous Solutions

temperature / °C	phase	$\rho_{\text{H}_2\text{O}}$	C_{NaOH}/M	phase	$\rho_{\text{H}_2\text{O}}$	C_{NaOH}/M
44.3	L	103	1.2	H	1.2	0.012
34.5	L	98.8	1.1	H	1.25	0.019
29.8	L	96	1.3	H	1.24	0.011

of temperature from crossing points of the dashed lines ($t = 19, 30, 34, 40$, and 44 °C) and the black dotted horizontal line ($C_{\text{NaCl}} = 1$ M) in Figure 2. The orange open diamonds in Figure 1 show the $\rho_{\text{H}_2\text{O}}$ values obtained in the manner mentioned above and converge to $\rho_{\text{H}_2\text{O}}^{\text{S}} = 42.7$ at $t = 25.7$ °C. Thus it can be said that the point where $\rho_{\text{H}_2\text{O}}^{\text{S}} = \rho_{\text{H}_2\text{O}}$ (about 42.7) exists at 25.7 °C for the L-phase solution with $C_{\text{NaCl}} = 1$ M. The NaCl concentration of the H-phase solution separated from the L-phase solution with $C_{\text{NaCl}} = 1$ M should be lower than 1 M (probably about 0.2 M).

Concentrations of NaOH in the phase-separated NIPA solutions obtained in dissolving the NIPA solid in the 1 M NaOH aqueous solutions are measured although NIPA molecules are partly hydrolyzed in the L-phase. The results are tabulated in Table 2. Most of NaOH molecules are distributed in the L-phase, and the $\rho_{\text{H}_2\text{O}}$ value of the L-phase is larger than that in the salt-free case when the temperature is the same. The red open triangles in Figure 1 representing the $\rho_{\text{H}_2\text{O}}$ value of the NIPA solution with $C_{\text{NaOH}} = 0.1$ M also show a larger $\rho_{\text{H}_2\text{O}}$ value than that in the salt-free case. This could be caused by a strong attractive interaction between NaOH and H₂O in the L-phase solution.

The phase-separation boundaries (cloud point curves) in the solutions with $C_{\text{HCl}} = 1.5$ M (blue open squares), 2.0 M (blue open circles), and 2.2 M HCl (blue open triangles) obtained from the observations of cloud points are shown in Figure 1. It should be mentioned that a cloud point of ($t, \rho_{\text{H}_2\text{O}}$) is the phase-separating onset t of the solution with $\rho_{\text{H}_2\text{O}}$, which should be the phase-separating H-phase or L-phase. It is noticeable that the plait points are observed at $\rho_{\text{H}_2\text{O}} = 3$ in the data of solutions with

Table 3. Concentrations of HCl, C_{HCl} , in the Phase-Separated NIPA Solutions Obtained upon Dissolving NIPA Solid in 2 M HCl Aqueous Solutions

temperature / °C	phase	$\rho_{\text{H}_2\text{O}}$	C_{HCl}/M	phase	$\rho_{\text{H}_2\text{O}}$	C_{HCl}/M	α^a
26	L	19.1	0.43	H	1.55	0.86	−0.34
	L	16.4	0.87	H	1.84	1.57	−0.33
	L	12.6	1.32	H	2.42	2.11	−0.34
	L	8.6	1.71	H	3.6	2.21	−0.35
	L	6.8	1.84	H	4.57	2.08	−0.36
30	L	17.8	0.84	H	1.82	1.54	−0.31
	L	14.2	1.25	H	2.33	2.06	−0.32
	L	20.9	0.42	H	1.54	0.81	−0.33
	L	7.4	1.94	H	4.53	2.18	−0.28
33.3	L	11	1.81	H	3.1	2.56	−0.32
34.7	L	15.7	1.29	H	2.23	2.17	−0.32
44.3	L	14.1	1.76	H	2.69	2.88	−0.35

^a $\alpha = \ln(C_{\text{HCl}}^{\text{L}}/C_{\text{HCl}}^{\text{H}})/\ln[(\rho_{\text{H}_2\text{O}}^{\text{L}} + 1)/(\rho_{\text{H}_2\text{O}}^{\text{H}} + 1)]$, where the superscripts “L” and “H” indicate the L- and H-phases.

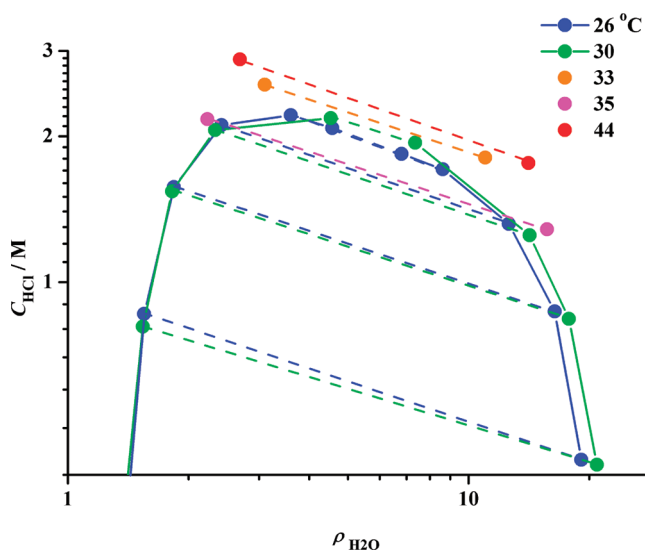


Figure 3. Distributions of HCl and H₂O between the separated phases of the solutions obtained upon dissolving the NIPA solid in HCl aqueous solutions with various concentrations at various temperatures indicated in the panel. Data are shown in Table 3. The dashed lines represent the tie lines, and the solid lines are guides for the eye.

$C_{\text{HCl}} = 2.0$ and 2.2 M. A boundary between the H-phase and the L-phase solutions might be $\rho_{\text{H}_2\text{O}} = 3$.

Concentrations of HCl in the phase-separated NIPA solutions obtained upon dissolving the NIPA solids in HCl aqueous solutions are tabulated in Table 3 and are plotted as functions of $\rho_{\text{H}_2\text{O}}$ in Figure 3. The concentration of HCl in the H-phase solution ($C_{\text{HCl}}^{\text{H}}$) is higher than that of the L-phase solution ($C_{\text{HCl}}^{\text{L}}$) equilibrating with the H-phase solution and the ratio of the former to the latter decrease with an increase in $\rho_{\text{H}_2\text{O}}^{\text{H}}/\rho_{\text{H}_2\text{O}}^{\text{L}}$, where $\rho_{\text{H}_2\text{O}}^{\text{H}}$ and $\rho_{\text{H}_2\text{O}}^{\text{L}}$ are the $\rho_{\text{H}_2\text{O}}$ values of the corresponding H-phase and L-phase, respectively. From the data shown in Table 3, the $\ln(C_{\text{HCl}}^{\text{L}}/C_{\text{HCl}}^{\text{H}})/\ln[(\rho_{\text{H}_2\text{O}}^{\text{L}} + 1)/(\rho_{\text{H}_2\text{O}}^{\text{H}} + 1)]$ value can be inferred to be a constant (-0.33 ± 0.02), from which the

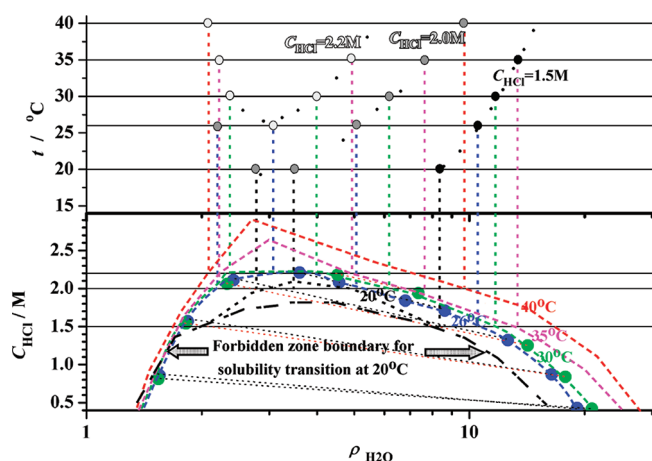


Figure 4. Schematic relation between the $C_{\text{HCl}}-\rho_{\text{H}_2\text{O}}$ phase map (curves of dashed lines in the lower panel) and the phase separation boundary of NIPA–HCl solution (filled and open circles in the upper panel) in the $t-\rho_{\text{H}_2\text{O}}$ diagram at $C_{\text{HCl}} = 1.5$ M (filled circles), 2.0 M (gray circles), and 2.2 M (open circles). The $C_{\text{HCl}}-\rho_{\text{H}_2\text{O}}$ relations at temperatures $t = 20$ °C (the black dashed line), 26 °C (the blue dashed line), 30 °C (the green dashed line), 35 °C (the pink dashed line), and 40 °C (the red dashed line) are presented in the lower panel. Blue ($t = 26$ °C) and green (30 °C) filled circles in the lower panel represent the experimentally obtained $(\rho_{\text{H}_2\text{O}}, C_{\text{HCl}})$ points. Dotted lines in the lower panel represent the tie lines. No solution with a composition of $(\rho_{\text{H}_2\text{O}}, C_{\text{HCl}})$ within the zone below the dotted and dashed line exists at $t = 20$ °C. The vertical dashed lines represent the correspondent relation between the points in the $C_{\text{HCl}}-\rho_{\text{H}_2\text{O}}$ phase map and the $t-\rho_{\text{H}_2\text{O}}$ diagram.

relation $3 \ln C_{\text{HCl}}^{\text{L}} - \ln X_{\text{NIPA}}^{\text{L}} = 3 \ln C_{\text{HCl}}^{\text{H}} - \ln X_{\text{NIPA}}^{\text{H}}$ or $X_{\text{NIPA}}^{\text{L}} = B(C_{\text{HCl}}^{\text{L}})^3$; $X_{\text{NIPA}}^{\text{H}} = B(C_{\text{HCl}}^{\text{H}})^3$ can be reduced. Here, the approximated relation, $X_{\text{NIPA}} \approx (\rho_{\text{H}_2\text{O}} + 1)^{-1}$ is used for the mole fraction of NIPA, X_{NIPA} , because $C_{\text{HCl}}/55.6 \ll 1$. The relation $\delta \ln X_{\text{NIPA}} = 3\delta \ln C_{\text{HCl}}$ derived from $3 \ln C_{\text{HCl}}^{\text{L}} - \ln X_{\text{NIPA}}^{\text{L}} = 3 \ln C_{\text{HCl}}^{\text{H}} - \ln X_{\text{NIPA}}^{\text{H}}$ indicates that the fluctuating entropy of the NIPA molecule is phenomenologically equal to 3 times that of HCl in the phase separation equilibrium. It is important to mention that the $\rho_{\text{H}_2\text{O}}$ value (about 5.7) of critical points at $t = 26$ and 30 °C shown in Figure 3 are different from the $\rho_{\text{H}_2\text{O}}$ value (about 3) of plait points shown in Figure 1. At the critical point, the fluctuation of the quantity of $X_{\text{NIPA}} (\propto C_{\text{HCl}}^3)$, which could be examined by the light scattering experiment, is maximal. It is noteworthy that the H-phase solution has a much stronger affinity for HCl than the L-phase solution. This could be caused by the attractive interaction between NIPA and HCl.

4. DISCUSSIONS

4.1. Cloud Boundary $t-\rho_{\text{H}_2\text{O}}$ Diagram and Phase-Separation $C_{\text{HCl}}-\rho_{\text{H}_2\text{O}}$ Map. Figure 4 schematically depicts the relation between the $C_{\text{HCl}}-\rho_{\text{H}_2\text{O}}$ phase map at $t = 20, 26, 30,$ and 40 °C (the lower panel) and the cloud boundaries of NIPA–HCl solution in the $t-\rho_{\text{H}_2\text{O}}$ diagram at $C_{\text{HCl}} = 1.5, 2.0,$ and 2.2 M (the upper panel). In the lower panel, the curves of blue and green dashed lines connecting the blue and green filled circles, the data of which are experimentally obtained and are shown in Figure 3, are the $C_{\text{HCl}}-\rho_{\text{H}_2\text{O}}$ relations at $t = 26$ and 30 °C, respectively. The curves of black, pink and red dashed lines in the lower panel represent the virtual $C_{\text{HCl}}-\rho_{\text{H}_2\text{O}}$ relations at $t = 20, 35,$ and 40 °C. The points at which the dashed lines described above intersect the horizontal lines representing $C_{\text{HCl}} = 1.5, 2.0,$

and 2.2 M in the lower panel are plotted as filled black, filled gray, and open circles in the upper panel of Figure 4. The vertical dashed lines (black: $t = 20$ °C; blue: $t = 26$ °C; green: $t = 30$ °C; pink: $t = 35$ °C; red: $t = 40$ °C) connecting the lower and the upper panels represent the correspondence between the $C_{\text{HCl}}-\rho_{\text{H}_2\text{O}}$ and the $t-\rho_{\text{H}_2\text{O}}$ relations. A transparent NIPA solution with $C_{\text{HCl}} = 1.5$ M and $r_{\text{H}_2\text{O}} = 8.4$ becomes turbid due to the onset of the separation of H-phase solution with a higher HCl concentration than 1.5 M and a $r_{\text{H}_2\text{O}}$ value lower than $\rho_{\text{H}_2\text{O}} = 8.4$ when the temperature reaches 20 °C upon heating the solution. The solutions with $C_{\text{HCl}} = 1.5$ M and a higher $r_{\text{H}_2\text{O}}$ value than 8.4 (e.g., $r_{\text{H}_2\text{O}} = 10.5, 11.9,$ or 13.5) can also become turbid at a higher temperature than 20 °C (e.g., $t = 26, 30,$ or 35 °C) in heating. The phase-separating temperatures, $t = 20, 26, 30,$ and 35 °C, as a function of $\rho_{\text{H}_2\text{O}}$ give the $t-\rho_{\text{H}_2\text{O}}$ relation of the phase separation boundary of the solutions with $C_{\text{HCl}} = 1.5$ M, as shown by the filled circles in the upper panel of Figure 4. In the same manner as described above, we can obtain the $t-\rho_{\text{H}_2\text{O}}$ relations of the phase separation boundaries of the solutions with 2.0 and 2.2 M HCl, as shown by the gray filled circles and open circles in the upper panel of Figure 4. In the case of $C_{\text{HCl}} = 1.5$ M, the curve of the $C_{\text{HCl}}-\rho_{\text{H}_2\text{O}}$ relation at $t = 20$ °C crosses over a forbidden zone boundary for the solubility transition. The $\rho_{\text{H}_2\text{O}}$ value at the crossing point should be the $\rho_{\text{H}_2\text{O}}^{\text{S}}$ of saturated solutions. The experimental result of the solution with $C_{\text{HCl}} = 1.5$ M indicates that the crossing points of $\rho_{\text{H}_2\text{O}}$ at $t = 22.8$ and 18.5 °C, respectively, are 1.9 and 8.3. The $t-\rho_{\text{H}_2\text{O}}$ relation of the phase separation boundary of the solution with 2.0 M HCl (blue open circles) shown in Figure 1 is considered to reflect the situation that the curve of $C_{\text{HCl}}-\rho_{\text{H}_2\text{O}}$ is tangent to the forbidden zone boundary at about 19.5 °C.

The $t-\rho_{\text{H}_2\text{O}}$ relation of the cloud boundary of the solutions with 1 M NaCl shown in Figure 1 reflects the $C_{\text{NaCl}}-\rho_{\text{H}_2\text{O}}$ relation shown in Figure 2, which can be approximately described by the equation $\rho_{\text{H}_2\text{O}} \approx \rho_0 \exp(C_{\text{NaCl}}/A)$. The values of ρ_0 are temperature independent in the H-phase and temperature dependent in the L-phase. The A values of -1.0 in the H-phase and 1.39 in the L-phase are independent of the temperature in both the H-phase and the L-phase. The negative and positive signs of $(\rho_{\text{H}_2\text{O}} - \rho_0)$ values indicate that Na^+ and Cl^- ions in the H-phase and the L-phase, respectively, seem to repel and attract H_2O molecules. Most of H_2O molecules form hydrogen bonds to the amide group of NIPA molecules in the H-phase solution, and a large portion of H_2O molecules forms the hydrophobic hydration networks in the L-phase solution. It could be inferred from the situation mentioned above that the state energy of the H_2O molecules hydrating NaCl with the formation of hydrogen bonds to the amide group is higher than the state energy of the H_2O molecules hydrating NaCl in the hydrophobic hydration network.

4.2. Effects of the Interactions of Ions with the Amide Group. Recent molecular dynamics simulations of poly(*N*-isopropylacrylamide)⁷ and *N*-methylacetamide²¹ in aqueous solutions of salts have exhibited that the Na cation has a strong affinity for the carbonyl oxygen of the amide group, and that the Cl anion has a very weak affinity for the amide hydrogen but has the tendency to be attracted by the hydrophobic hydration network. The simulations have been carried out for the H_2O -rich cases, which correspond to the L-phase solution in the present experiments, and cannot reveal much about the H-phase solution. From the present experimental result that most of the Na^+ and OH^- ions in the phase-separated NIPA solutions are distributed in the L-phase, it can be inferred that Na^+ and

OH[−] ions are very stabilized in the hydrated state that hardly exists in the H-phase solution, where most of the carbonyl oxygens of the amide groups form hydrogen bonds to H₂O molecules and cannot directly interact with the Na cation. The Na cations hydrated in the L-phase are much more stabilized than the NaOH ion-pairs dehydrated in the H-phase even when they are distributing near the carbonyl oxygens of the amide group. The situation that the hydrated Na cation in the L-phase solution is more stabilized than the NaCl ion-pairs in the H-phase solution can be inferred from the result shown in Table 1 indicating more Na⁺ and Cl[−] ions distributing in the L-phase solution than those in the H-phase solution.

The simulation⁷ has exhibited the affinity of a Cl anion for the methyl group and weak interaction between the Cl anion and the amide group. The possible explanation for more HCl distributing in the H-phase of phase-separated NIPA solutions is as follows. The hydronium ion, H₃O⁺ distributed around the amide group can form an ion-pair with the Cl anion that is distributed around the methyl group and the vinyl group in the H-phase. Many H₂O molecules surround the H₃O⁺ and the Cl anion in the L-phase and interfere with the ion-pair formation.^{22,23} The formation of the ion-pair could lower the state energy of HCl in the H-phase solution by the Coulomb energy of the H₃O⁺ and the Cl anion. The distribution of Cl anion around the vinyl group can give the amphiphilic nature to the vinyl group and improve the NIPA solubility in the water. The phase-separation map of NIPA in the 2.2 M HCl solution shown in Figure 1 is in fact similar to the phase-separation diagram of *N*-(isopropyl)propionamide,¹³ in which the vinyl group is replaced by a less hydrophobic ethyl group.

5. CONCLUSIONS

We examined changes in the solubility transition and the phase-separation behavior of NIPA solution with additions of NaCl, NaOH, and HCl and found differences in the effect on the dissolved state of NIPA molecule in water between Na cation and Cl anion. The solubility change of NIPA in the salt-free water at the solubility transition¹⁸ decreases with an increase in HCl concentration and disappears at HCl concentrations higher than 2M, while it increases with increases in NaOH and NaCl concentrations. A temperature of the solubility transition decreases with an increase in HCl concentration and increases with increases in NaOH and NaCl concentrations. Partition coefficients of HCl in the phase-separated NIPA-rich solutions are higher than those in the NIPA-poor solutions, while partition coefficients of NaCl and NaOH between the NIPA rich and poor solutions have trends opposite to those of HCl. The present results demonstrate that Na cation stabilizes the hydrated state of NIPA molecule and that the Cl anion stabilizes the dehydrated state of NIPA molecules.

AUTHOR INFORMATION

Corresponding Author

*Tel & Fax: +81-92-642-2609. E-mail: shigeo-ssk@chem.kyushu-univ.jp or famssk@clock.ocn.ne.jp.

REFERENCES

- (1) Omta, A. W.; Kropman, M. F.; Woutersen, S.; Bakker, H. J. *Science* **2003**, *301*, 347–349.
- (2) Omta, A. W.; Kropman, M. F.; Woutersen, S.; Bakker, H. J. *J. Chem. Phys.* **2003**, *119*, 12457–12461.
- (3) Hofmeister, F. *Arch. Exp. Pathol. Pharmacol.* **1888**, *24*, 247–260.

- (4) Kunz, W.; Henle, J.; Ninham, B. W. *Curr. Opin. Colloid Interface Sci.* **2004**, *9*, 19–37.
- (5) Boström, M.; Williams, D. R. M.; Ninham, B. W. *Phys. Rev. Lett.* **2001**, *87*, 168103.
- (6) Zhang, Y.; Foryk, D.; Bergbreiter, D. E.; Cremer, P. S. *J. Am. Chem. Soc.* **2005**, *127*, 14505–14510.
- (7) Du, H.; Wickramasinghe, R.; Qian, X. *J. Phys. Chem. B* **2010**, *114*, 16594–16602.
- (8) Zhang, Y.; Cremer, P. S. *Curr. Opin. Chem. Biol.* **2006**, *10*, 658–663.
- (9) Dušek, K. Ed. *Responsive Gels: Volume Transitions I (Advances in Polymer Science)*; Springer: New York, 1993; Vol. 109.
- (10) Dušek, K. Ed. *Responsive Gels: Volume Transitions II (Advances in Polymer Science)*; Springer: New York, 1993; Vol. 110.
- (11) Koga, S.; Sasaki, S.; Maeda, H. *J. Phys. Chem.* **2001**, *105*, 4105–4110.
- (12) Afroze, F.; Nies, E.; Berghmans, H. *J. Mol. Struct.* **2000**, *554*, 55–68.
- (13) Geukens, B.; Meersman, F.; Nies, E. *J. Phys. Chem. B* **2008**, *112*, 4474–4477.
- (14) Kawasaki, H.; Mitou, T.; Sasaki, S.; Maeda, H. *Langmuir* **2000**, *16*, 1444–1446.
- (15) Gill, S. J.; Dec, S. F.; Olofsson, G.; Wadsö, I. *J. Phys. Chem.* **1985**, *89*, 3578–3761.
- (16) Paschek, D. J. *Chem. Phys.* **2004**, *120*, 10605–10617.
- (17) Tiktupulo, E. I.; Uversky, V. N.; Luschchik, V. B.; Klenin, S. I.; Bychkova, V. E.; Ptitsyn, O. B. *Macromolecules* **1995**, *28*, 7519–7524.
- (18) Sasaki, S.; Okabe, S.; Miyahara, Y. *J. Phys. Chem. B* **2010**, *114*, 14995–15002.
- (19) Pan, B.; Ricci, M. S.; Trout, B. L. *J. Phys. Chem. B* **2011**, *115*, 5958–5970.
- (20) Smith, R. M.; Hansen, D. E. *J. Am. Chem. Soc.* **1998**, *120*, 8910–8913.
- (21) Heyda, J.; Vincent, J. C.; Tobias, D. J.; Dzubiella, J.; Jungwirth, P. *J. Phys. Chem. B* **2010**, *114*, 1213–1220.
- (22) Xu, J.; Izvekov, S.; Voth, G. A. *J. Phys. Chem. B* **2010**, *114*, 9555–9562.
- (23) Wang, F.; Izvekov, S.; Voth, A. G. *J. Am. Chem. Soc.* **2008**, *130*, 3120–3126.